Science and Technology Indonesia
e-ISSN:2580-4391 *p*-ISSN:2580-4405
Vol. 8, No. 2, April 2023

Research Paper

Preparation of Al_2O_3/PVA Nanocomposite Thin Films by a Plasma Jet Method

Saba Jawad Kadhem[1]*

[1]*Department of Physics, College of Science, University of Baghdad, Baghdad, 10071, Iraq*
***Corresponding author**: saba.kadhem@sc.uobaghdad.edu.iq

Abstract
Alumina thin films have significant applications in the areas of optoelectronics, optics, electrical insulators, sensors and tribology. The novel aspect of this work is that the homogeneous alumina thin films were prepared in several stages to generate a plasma jet. In this paper, aluminium nanoparticles suspended in vinyl alcohol were prepared using exploding wire plasma. TEM analysis was used to determine the size and shape of particles in aluminium and vinyl alcohol suspensions; the TEM images showed that the particle size is 17.2 nm. Aluminium/poly vinyl alcohol (Al/PVA) thin films were prepared using this suspension on quartz substrate by plasma jet technique at room temperature with an argon gas flow rate of 1 L/min. The Al/PVA thin films were thermally converted to alumina films, where they were annealed at different temperatures (700, 800, or 900°C). X-ray diffraction (XRD), atomic force microscopy (AFM), transmission electron microscopy (TEM), scanning electron microscopy (SEM), and Fourier transform infrared spectroscopy (FTIR) techniques were used to characterise these thin films before and after annealing process. The diffraction patterns of the prepared thin films before subjecting them to the annealing process indicated the presence of peaks belonging to aluminium and PVA; however, the diffraction patterns and FTIR spectra obtained for these films after the annealing process showed peaks indicating the formation of alumina films of different phases. AFM and SEM investigations proved that the formed particles for all prepared films before and after the annealing process were similar in size and almost spherical; the diameter of the particles was on the order of a few nanometres. To control the properties of prepared thin films, the plasma which was used to produce thin films is diagnosed spectrophotometrically. The generated plasma was diagnosed using optical emission spectroscopy to estimate the electron temperature Te; the electron temperature was 1.925 eV.

Keywords
Al/PVA Nanocomposite, Al_2O_3 Thin Film, Plasma Jet, Alumina, Annealing Effect

Received: 10 March 2023, Accepted: 15 June 2023
https://doi.org/10.26554/sti.2023.8.2.471-478

1. INTRODUCTION

Recently, simple metal oxide powders with nanoscale dimensions have received much attention because of their importance in industrial applications (Arat et al., 2018). Simple oxides, such as Al_2O_3, are an important class of nanoparticles (NPs) that are used in many industrial fields such as water absorption, wastewater treatment, electrical insulators, catalyst supports or catalysts, coarse, structural composites for spacecraft applications, thermal wear coatings, and thin-film coatings (Sugumaran et al., 2015; He et al., 2016; Segawa et al., 2014). Al_2O_3 thin films have attracted rising interest due to the unique thermal, electrical, mechanical, magnetic, and optical properties that nanocomposites display. Because of the nano-size of these particles, their chemical and physical properties are much different from those of bulk materials (Segawa et al., 2014).

Synthetic poly (vinyl alcohol) (PVA) is largely produced for its wide practical applications resulting from its unique physical properties and chemical resistance. PVA is a linear polymer with a semi-crystalline structure and is soluble in water (Segawa et al., 2014; Dhawale et al., 2018; Yang et al., 2015; Bhargav et al., 2007). PVA was chosen because of its unique ability to form homogeneous films, good processability, and good chemical resistance. It is a soluble crystalline structure that is easily degradable in water (Yadav and Bajpai, 2018). In this work, PVA and Al were mixed to produce Al/PVA thin films using plasma polarization. PVA was chosen to mix with aluminium because it is a good host material due to its chemical resistance, good thermal stability, and film-forming ability (Bhargav et al., 2007; Yadav and Bajpai, 2018; Fan et al., 2020). To prepare liquid containing aluminium NPs suspended in vinyl alcohol monomer, an electric exploding wire technique was used (Fan et al., 2020; Alsaad et al., 2021; Tang et al., 2015). This method is considered one of the most environmentally friendly methods for preparing NPs of metallic materials (Tang et al., 2015; Hussein and Kadhem, 2021; Abdulla et al., 2022; Bai

et al., 2019; Tanaka et al., 2021; Ghorbani, 2014; Abbass and Kadhem, 2018). To produce Al/PVA films, a plasma jet system was used because it is an easy, inexpensive, and efficient way to produce thin films (Abbass and Kadhem, 2018; Nikiforov et al., 2015; Gencer et al., 2008). There are several techniques for preparing thin films such as the coating and sputtering, direct current plus pulse (DCP) method, Sol–Gel technique and casting method, but the plasma Jet system is a very good tool for producing stable and high homogeneous film (Sathish and Shekar, 2012; Mikailzade et al., 2018; Sugumaran et al., 2015; Goktas and Goktas, 2021; Riyadh et al., 2020; Zhao et al., 2014). The unique advantages of the Plasma Jet thin film deposition system are that it compared with other methods are an easy-to-use system, the properties of prepared film can be controlled by controlling the plasma parameters, the area of the thin film and its location on the substrate can be controlled, the films prepared by this technique are very homogeneous and single-layer or multi-layer films can be prepared easily using the plasma jet system.

A plasma jet is a type of non-thermal, atmospheric, capacitively coupled glow discharge. It has a one-electrode configuration and is operated with argon gas (Mohammed et al., 2022; Abed, 2018; Ussenov et al., 2021). The important advantages of this system are that it is small and lightweight with a compact design. It is easy to use and can be constructed from cheap, readily available components (Huang et al., 2018; Kinandana et al., 2018; Jung et al., 2022). This research demonstrates the possibility of changing the characteristics of the Al/PVA films by an annealing process to obtain Al_2O_3 thin films and improve their general performance (Lee, 2013; Baggetto et al., 2015; Parauha et al., 2021). Nanocomposites containing Al_2O_3 have superior properties such as good chemical stability, moderate-to-high mechanical strength, and high thermal resistance (Chunduri et al., 2014). The novelty of using a plasma jet method for the preparation of nanocomposite thin films is characterized by two aspects. Firstly, the system is designed to enable the automatic movement of the plasma torch nozzle in both the x and y directions over the slide where the film is deposited. This design ensures an even distribution of the suspended colloid mixed with the gas on the substrate. Secondly, the plasma jet method involves the utilization of a highly energetic plasma jet, typically generated by a plasma torch, to deposit thin films onto substrates. This technique offers several advantages over conventional deposition methods, such as improved film quality, control over film thickness, and enhanced homogeneity.

The unique characteristics of the plasma jet, including its high temperature, high kinetic energy, and ionization capabilities, enable efficient interactions between the precursor material and the substrate surface. These interactions promote the formation of a dense and uniform film, overcoming challenges associated with defects, non-uniformity, and impurities commonly encountered in other deposition techniques. This research aims to investigate the plasma jet-assisted preparation of Al/PVA thin films, followed by their annealing to obtain homogeneous alumina thin films. The prepared thin films have been characterized using various analytical techniques, including Fourier transform infrared spectroscopy (FTIR), UV-visible spectroscopy, X-ray diffraction (XRD), scanning electron microscopy (SEM), and atomic force microscopy (AFM).

2. CHEMICAL MATERIALS

- Vinyl alcohol (VA) monomer : Vinyl alcohol (VA) is an organic compound with the chemical formula CH_2=CHO H. It has a vinyl group (CH_2=CH-) attached to a hydroxyl group (-OH). This structure makes it highly reactive and prone to undergoing polymerization reactions. Vinyl alcohol is a polar molecule due to the presence of the hydroxyl group, making it water-soluble and capable of forming hydrogen bonds. It is colorless, and its density 0.943 (g/cm^3) .Manufactured from panreac corn Co., Ltd., Spain.
- Aluminium: High purity aluminium plate and wire (99.9 8%). The plate has a length of 3 cm and a width of 2 cm, with a thickness of 2 mm. The wire measures 15 cm in length and has a diameter of 0.3 mm.
- Argon gas: to generate plasma jet.

3. INSTRUMENTS

- A.C. Power supply: high voltage 10 kV and a cut frequency of 28 kHz.
- D.C. power supply: with high current (1-250A) and voltage 80 volt .

4. EXPERIMENTAL TECHNIQUES

4.1 Preparing Aluminium/Vinyl Alcohol Colloid

Aluminium NPs suspended in 100 mL of vinyl alcohol monomer were prepared via the hybrid method, which is a combination of the spark discharge method and the exploding wire method. Two electrodes were used, the first was an aluminium wire connected to the negative pole of the power supply, and the second was an aluminium plate connected to the positive pole. The electrodes were immersed in 100 mL of vinyl alcohol monomer. The two electrodes will melt and vaporize and turn into plasma when the wire touches the Al plate and a high current (75 A) passes through the electrodes. The metallic plasma forms and expands at a supersonic speed creating shock waves in the surrounding medium. The plasma is cooled when it interacts with the surrounding liquid and then NPs are formed through a nucleation process. Finally, the colloid is extracted and deposited in the form of films using the plasma jet system.

The generated plasma was diagnosed using optical emission spectroscopy (OES) to determine the temperature of the electrons. The diagnosis was carried out for plasmas generated with three values of argon gas flow rate (5, 10, and 15) L/min.

4.2 Al/PVA Thin Film Preparation

The schematic diagram of the plasma jet device for fabrication of thin films in liquid media is shown in Figure 1. The films

were deposited by an atmospheric plasma jet. The generated plasma was directed downstream to a glass substrate which was positioned 2.5 cm from the end of the plasma needle. The plasma torch was generated via Ar gas (with a flow rate of 0.5 L/min) passing through the aluminium/vinyl alcohol colloid inside a nebulizer.

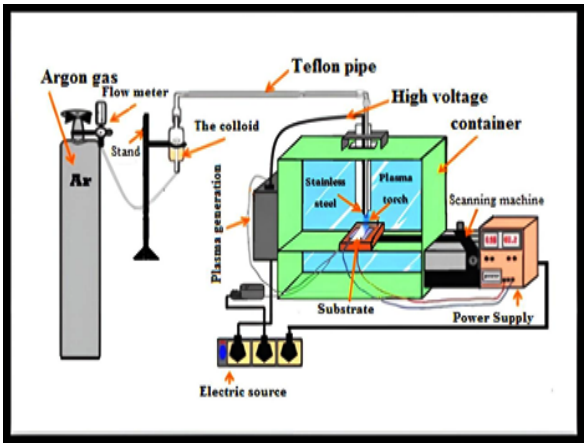

Figure 1. The Schematic Diagram of the Plasma Jet System

The aerosol was guided by the argon gas through a Teflon pipe to the plasma jet system. The plasma was ignited using an electric source with a frequency of 28 kHz. The glass slide was placed on a base that is movable in two orthogonal directions to obtain very uniform films. The prepared thin films were annealed at 700, 800, or 900°C in a vacuum environment for 1 hour. Structural analysis of the thin films was performed by XRD diffraction with scanning angles (2θ) from 19° to 80°. The crystallographic structure of samples before and after annealing treatment was evaluated to determine whether alumina had formed as well as to determine the phase of the alumina.

The morphology and roughness of the film surfaces were tested by atomic force microscopy (AFM) before (for Al/PVA thin films) and after annealing (for Al_2O_3 thin films).

5. RESULTS AND DISCUSSIONS

5.1 Optical Emission Spectra

OES is a well-known method for reliably monitoring numerous characteristics of atmospheric pressure plasma jets. Optical emission spectra of the plasma sources are shown in Figure 2. The spectrum shows emission lines corresponding to a group of N_2 emissions including the second positive system N_2 at 316, 337, 358, 380, and 406 nm; first negative system N_2 at 391 and 428 nm; and OH at 306 nm. The emissions of OH and nitrogen are due to the presence of water vapour in the atmosphere.

Electron temperature (Te) can be calculated by the line-intensity-ratio method. The value R_1/R_2 is calculated from the spectra. The electron temperature (Te) can then be calculated using Equations (1) and (2) (Kinandana et al., 2018).

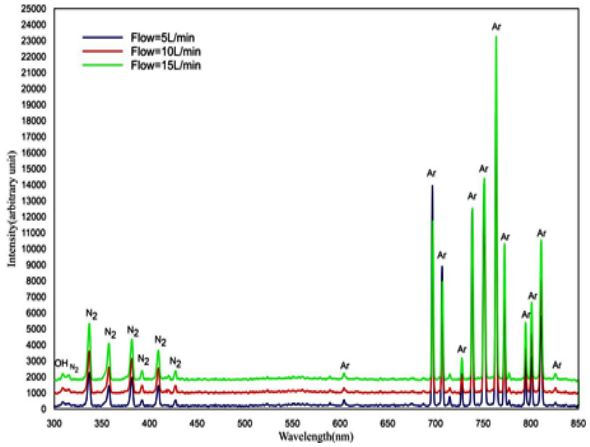

Figure 2. Emission Spectra of the Atmospheric Pressure Ar Plasma Jet at Different Flow Rates of Argon Gas (5, 10, and 15) L/min

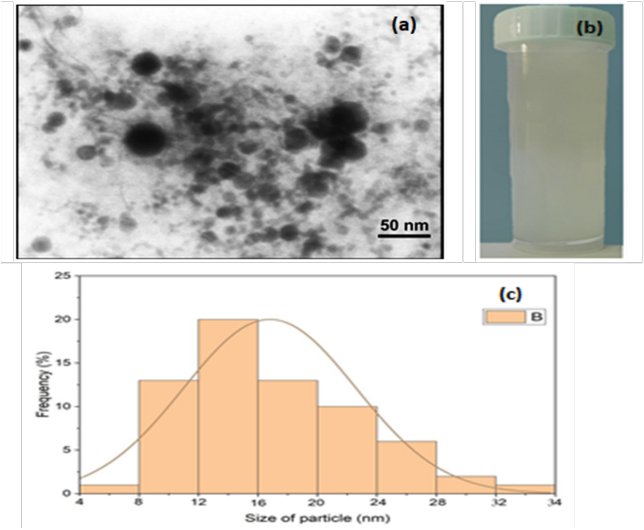

Figure 3. (a) TEM Image of Aluminium/Vinyl Alcohol Colloid, (b) Photo of Al/PVA Colloidal, (c) Particle-Size Histogram of Aluminium/Vinyl Alcohol Colloid Produced by Electrical Exploding Wire Method

$$\frac{R_1}{R_2} = \frac{\frac{I_1}{I_2}}{\frac{I_3}{I_4}} \quad (1)$$

$$\frac{R_1}{R_2} = 8.95 \times 10^{-5} \exp \frac{14.31}{kTe} \quad (2)$$

The R_1/R_2 values are 9.15, 9.8, and 9.8 at argon gas flow rates of 5, 10, and 15 L/min, respectively. This corresponds to an electron temperature of 1.925 eV where:

I_1, I_2 (belonging to N_1 lines) and I_3, I_4 (belonging to N_2) are the intensities of the lines with wavelengths of 381, 427,

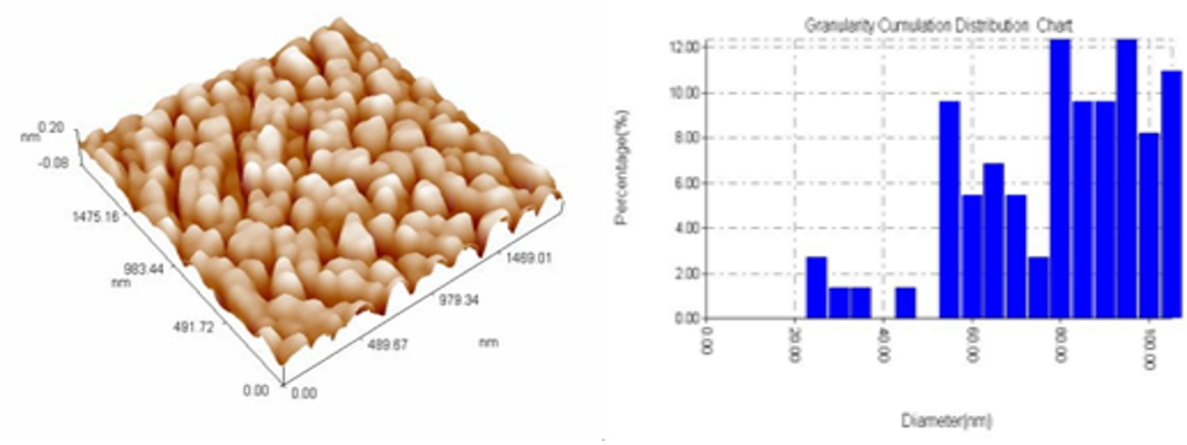

Figure 4. AFM Image (3D) and Distribution Chart of Synthesis of the Al/PVA Films Before Annealing

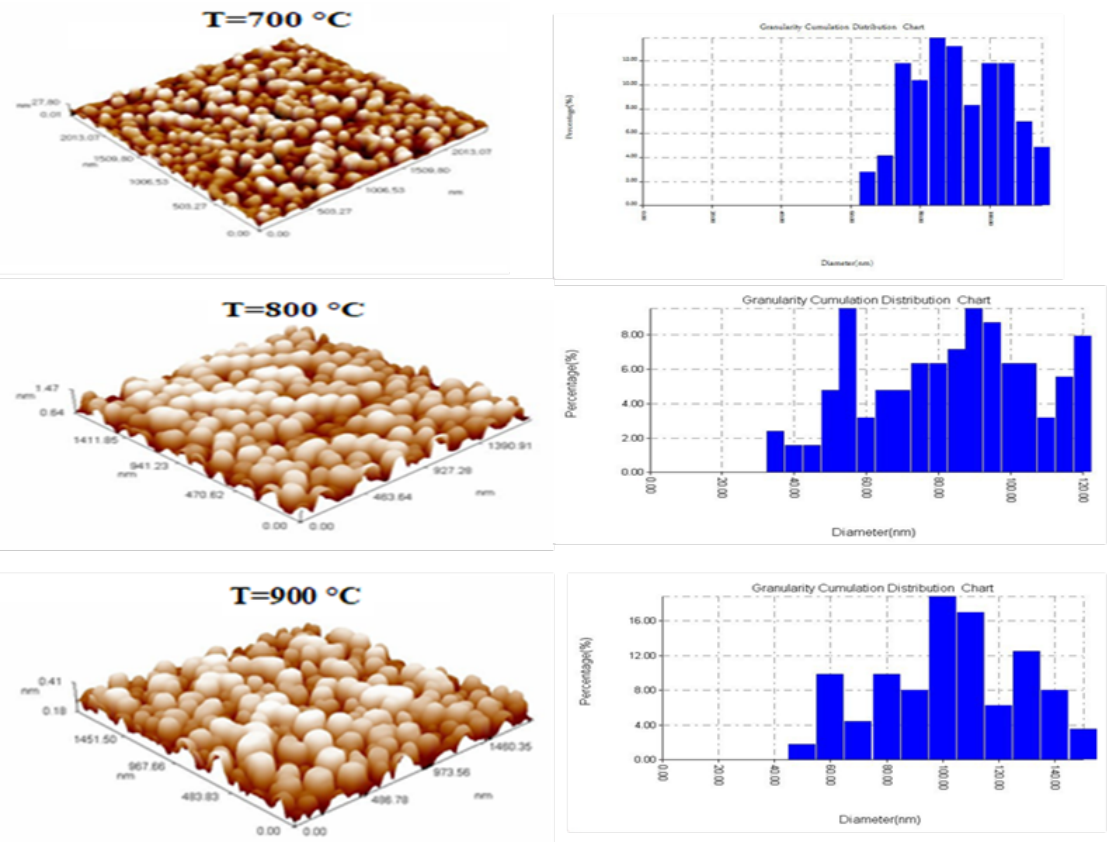

Figure 5. AFM Image (3D) and Distribution Chart of the Synthesis of the Al_2O_3 Films After Annealing at Different Temperatures

392, and 409 nm respectively. The temperature is about 330 K, which is about 60 times higher than the gas temperature when the electron temperature is comparable to that calculated and measured by the others (Abbass and Kadhem, 2018; Christova et al., 2004).

5.2 Transmission Electron Microscopy Analysis (TEM)

TEM analysis was performed to verify the creation of aluminium/vinyl alcohol colloid, as shown in Figure 3. The information pertinent to the size, form, and agglomeration was gained from TEM analysis. A transparent layer can be observed around the aluminium particles resulting from the polymerization of ethylene alcohol by the action of the plasma. The Image J software program was used to compute the particle

sizes within the TEM images. The average size of the aluminium NPs suspended in vinyl alcohol is 17.2 nm, as shown in the particle-size histogram in Figure 3-b.

5.3 Atomic Force Microscope (AFM) Analysis

In this work, AFM was used to determine surface topography, including the size and shape of the Al/PVA and Al_2O_3 NPs. Figure 4 shows the AFM images together with histograms of the particle-size distributions for Al/PVA thin films prepared using the plasma jet method at room temperature with a 1 L/min flow rate of argon gas. It is observed that the particles are nanosized with an average diameter of 76 nm and approximately spherical. The AFM images together with histograms of the particle-size distributions of alumina thin films are illustrated in Figure 5. It is noteworthy that the alumina NPs are small and uniform in size. The obtained films demonstrate a smooth surface with a small number of large particles, and the particles are homogeneously packed. A few agglomeration particles are observed with increasing annealing temperature. The average NP diameters of three alumina thin films that were annealed at 700, 800, and 900°C are 80.69, 86.14, and 96.2 nm, respectively. The size of the NPs increases with increasing annealing temperature because of coalescence between the particles.

5.4 X-Ray Diffraction Results for the Nanocomposite Thin Films

XRD studies in the range of 19°–80° were carried out to corroborate the crystallinity of the prepared nanocomposite films and to determine their crystal structure. Figure 6 shows the XRD pattern for Al/PVA nanocomposite films that were prepared with the plasma jet at a 1 L/min flow rate of argon gas. The main diffraction peaks are at 38.45°, 44.62°, and 64.99°, which can be assigned to diffractions from the (111), (200), and (220) aluminium planes, respectively. Diffraction peaks were also observed at 22.55° for the PVA compound. The broadness of the peaks in the XRD pattern is evidence that the particle sizes are in the nanoscale range. The mean crystallite size of Al/PVA nanocomposite film is 17.03.

Figure 7 presents the XRD patterns for Al_2O_3 thin films that were prepared using the plasma jet method at 1 L/min and then were annealed at 700, 800, or 900°C. For all samples, there are three diffraction peaks at 37.3°, 45.5°, and 66.4°, which can be assigned to diffractions from the (311), (400), and (440) alumina planes, respectively. From the diffraction patterns of the three samples, crystallization improves with increased annealing temperatures. When the samples were heated up to 700 or 800°C, the gamma phase of alumina (γ-) remained.

However, the samples were heated up to 900°C, the crystallization improved along with an increase in the size of the crystals. This means that by increasing the heating temperature, a conversion from γ-Al_2O_3 to α-Al_2O_3 occurs. These obtained results are in agreement with Dhawale et al. (2018). The diffraction pattern of the annealed samples is devoid of

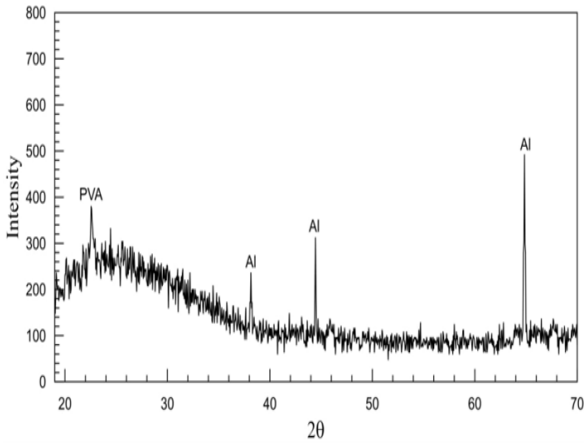

Figure 6. X-Ray Diffraction Pattern for Al/PVA Film Before Annealing

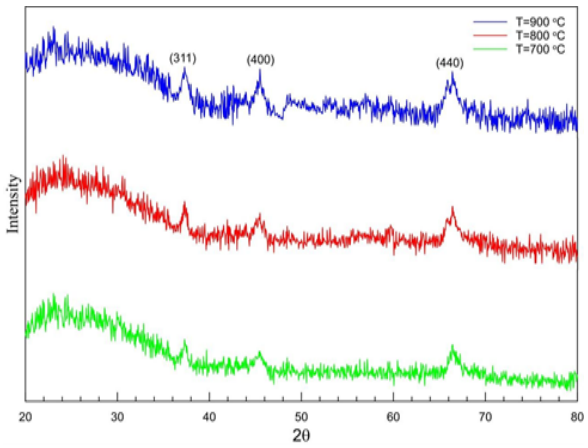

Figure 7. XRD Patterns for Al_2O_3 Films After Annealing at Different Temperatures

PVA peaks because of the dissociation of this compound at high temperatures.

Debye-Sherrer formula and full width at half maximum (FWHM) were used to estimate the mean crystallite size of Al_2O_3 nanoparticles according to equation (Shameli et al., 2012):

$$D = \left(\frac{(0.89\lambda)}{(B\cos\theta)} \right) \quad (3)$$

where, λ is the x-ray wavelength (1.5406 Å), 0.89 is the shape factor, B is full width at half maximum of the peak (FWHM), and θ is the Bragg angle. The mean crystallite size of three Al_2O_3 thin films that were annealed at 700, 800, and 900°C are around 15.23, 17.06 and 23.09 nm, respectively.

5.5 FT-IR Spectroscopy of Al/PVA Nanocomposite Thin Films

Figure 8 shows the FT-IR spectra of two samples of Al_2O_3 films synthesized via the plasma jet method at room temperature with an Ar gas flow rate of 1 L/min, followed by annealing of the first sample at 700°C and the second at 900°C in a vacuum environment for 1 hour. Two samples were analysed at two different temperatures to clearly show the effect of raising the temperature on the crystal structure of the samples. In Figure 8-a, there are two bands around 690.47 cm^{-1} and 1085.85 cm^{-1} that are related to the Al–O stretching mode in a tetrahedron and to the symmetric bending of Al–O–H, respectively. On the other hand, in Figure 8-b the bands around 692.40 cm^{-1} and 1081 cm^{-1} correspond to the Al–O stretching mode in a tetrahedron and to symmetric bending of Al–O–H. The wide absorbance bands between 900 and 1100 cm^{-1} are associated with O–H deformation vibrations. The appearance of sharp peaks in the spectrum confirms the presence of a good crystallization state. In Figure 8-a, there is a wide band at 3434.98 cm^{-1} which are related to O-H stretching because of the chaotic distribution of vacancies for γ-Al_2O_3 NPs. The appearance of this band is evidence of incomplete crystallization in the spectrum of the sample that was heated up to 900°C, bands appear at 466.74 cm^{-1}, 578.60 cm^{-1}, and 646.11 cm^{-1} that are related to the octahedral structure Al–O stretching mode. The appearance of these bands indicates a highly crystalline state of α-Al_2O_3 when the annealing temperature was increased. It is noteworthy in Figures (7-a) and (7-b) that the spectrum intensity in general decreases with increasing annealing temperature, which indicates the improvement of crystallization in the prepared film. The results are in agreement with Lee (2013).

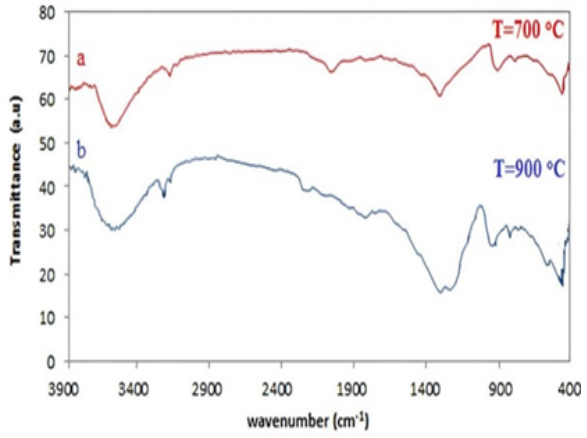

Figure 8. Typical FTIR Spectrum of Al_2O_3 at a: 700°C and b: 900°C Annealing Temperature

5.6 Scanning Electron Microscopy (SEM) Analyses

The morphology of the Al_2O_3 films synthesized by the plasma jet method and annealed at 700 or 900°C was explored by SEM, as shown in Figure 9. The SEM images establish that the formed particles had a nanoparticle nature and morphology, that the NPs agglomerated, and the complete separation was not achieved. The Al_2O_3 NPs in the fabricated films were nearly spherical, and their size increased as the annealing temperatures increased. The reason for the existence of some large particles that are sometimes clustered may be that some of the particles have a large surface area, causing weak attractive forces with small particles close to them. Moreover, since the samples are exposed to high temperatures during the annealing process, recombination of some of the closely spaced NPs may occur. This is consistent with what was obtained in the AFM analysis.

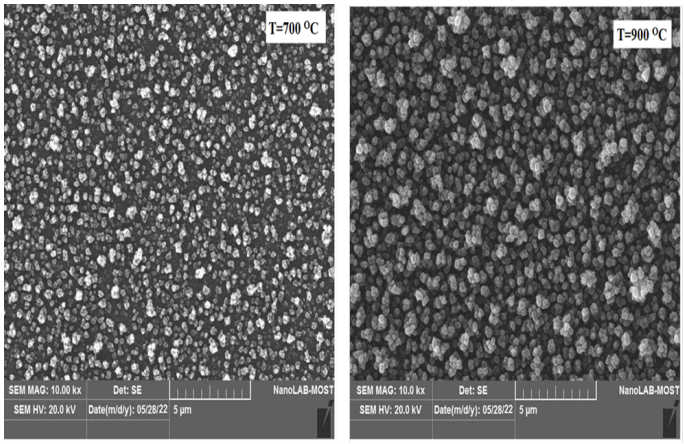

Figure 9. SEM Images of Al_2O_3 Films Produced by the Plasma Jet Technique After Annealing at 700°C or 900°C

6. CONCLUSION

High purity γ-Al_2O_3 and α-Al_2O_3 thin films were produced with atmospheric plasma jet technology, and their properties were confirmed by XRD and FTIR analysis. Very homogeneous thin films of different materials can be prepared with the plasma jet technique. The produced films were diagnosed by optical emission spectroscopy, and the temperature of the electrons (Te) was 1.925 eV. The exploding wire technique is a superior method for preparing an ideal suspension of aluminium NPs within a vinyl alcohol monomer. TEM images together with histograms of the particle-size distributions confirmed that the Al particles are approximately uniform, spherically shaped, and have a narrow size distribution within the few-nanometer range. The resultant nanofluid was deposited in the form of thin films by the plasma jet system. Finally, these thin films were annealed at different temperatures. The phases of alumina films (α-Al_2O_3 and γ-Al_2O_3) were distinguished by their FTIR spectra and X-ray diffraction patterns. AFM and SEM analysis images indicate that the prepared films are homogeneous with uniformly sized particles less than 100 nm in diameter.

7. ACKNOWLEDGMENT

The author wishes to express their gratitude to Plasma Physics Lab. members in Physics Department, College of Science, University of Baghdad.

REFERENCES

Abbass, A. and S. Kadhem (2018). Preparation and Characterization DLC Thin Films Using Atmospheric Pressure Plasma Jet. *IOP Conference Series: Materials Science and Engineering*, **454**(1); 012065

Abdulla, S. H., H. R. Humud, and F. I. Mustafa (2022). Preparation of a Composite of Copper Oxide Nanoparticles with Carbon by Exploding Graphite Rod in Aqueous Suspension. *Iraqi Journal of Physics*, **20**(1); 26–36

Abed, M. A. (2018). Aerosol Assisted Dielectric Barrier Discharge Plasma Jet for PMMA/ZnS Nanocomposite Thin Films Preparation. *University of Thi-Qar Journal of Science*, **2**(4); 158–162

Alsaad, A., A. Ahmad, A. R. Al Dairy, I. A. Qattan, S. Al Fawares, and Q. Al-Bataineh (2021). Characterization of As-Prepared (PMMA-PVA)/CuO-NPs Hybrid Nanocomposite Thin Films. *Polymer Bulletin*, **79**(4); 1–22

Arat, A. K., D. H. Abdulkadhim, and M. H. Rashid (2018). Study of Electrical Properties of Poly (Vinyl Alcohol)/Alumina (PVA/Al2O3) Nanocomposites. *Journal of University of Babylon for Pure and Applied Sciences*, **26**(6); 95–100

Baggetto, L., J. Esvan, C. Charvillat, D. Samélor, H. Vergnes, B. Caussat, A. Gleizes, and C. Vahlas (2015). Alumina Thin Films Prepared by Direct Liquid Injection Chemical Vapor Deposition of Dimethylaluminum Isopropoxide: A Process-Structure investigation. *physica Status Solidi (C)*, **12**(7); 989–995

Bai, J., Z. Shi, C. Huang, Z. Wu, and S. Jia (2019). Electrical Explosion of Aluminum Wire for Preparation of Nanoparticles: An Experimental Study. *Journal of Physics D: Applied Physics*, **52**(42); 425201

Bhargav, P. B., V. M. Mohan, A. Sharma, and V. N. Rao (2007). Structural, Electrical and Optical Characterization of Pure and Doped Poly (Vinyl Alcohol)(PVA) Polymer Electrolyte Films. *International Journal of Polymeric Materials*, **56**(6); 579–591

Christova, M., E. Castanos-Martinez, M. Calzada, Y. Kabouzi, J. Luque, and M. Moisan (2004). Electron Density and Gas Temperature from Line Broadening in an Argon Surface-Wave-Sustained Discharge at Atmospheric Pressure. *Applied Spectroscopy*, **58**(9); 1032–1037

Chunduri, L., T. M. Rattan, M. Molli, and V. Kamisetti (2014). Single Step Preparation of Nano Size Gamma Alumina Exhibiting Enhanced Fluoride Adsorption. *Materials Express*, **4**(3); 235–241

Dhawale, V. P., V. Khobragade, and S. D. Kulkarni (2018). Synthesis and Characterization of Aluminium Oxide (Al_2O_3) Nanoparticles and its Application in Azodye Decolourisation. *Chemistry*, **27**; 31

Fan, L., H. Zhang, M. Gao, M. Zhang, P. Liu, and X. Liu (2020). Cellulose Nanocrystals/Silver Nanoparticles: In-Situ Preparation and Application in PVA Films. *Holzforschung*, **74**(5); 523–528

Gencer, H., A. Goktas, M. Gunes, H. Mutlu, and S. Atalay (2008). Electrical Transport and Magnetoresistance Properties of $La_{0.67}Ca_{0.33}MnO_3$ Film Coated on Pyrex Glass Substrate. *International Journal of Modern Physics B*, **22**(05); 497–506

Ghorbani, H. R. (2014). A Review of Methods for Synthesis of Al Nanoparticles. *Oriental Journal of Chemistry*, **30**(4); 1941–1949

Goktas, S. and A. Goktas (2021). A Comparative Study on Recent Progress in Efficient ZnO Based Nanocomposite and Heterojunction Photocatalysts: A Review. *Journal of Alloys and Compounds*, **863**; 158734

He, L. J., L. Y. Wang, W. Z. Chen, and X. Z. Liu (2016). Thermal Conductivity of Alumina Films Prepared by Inclined Incidence. *Current Nanoscience*, **12**(5); 630–635

Huang, K. Y., H. Y. Chi, P. K. Kao, F. H. Huang, Q. M. Jian, I. C. Cheng, W. Y. Lee, C. C. Hsu, and D. Y. Kang (2018). Atmospheric Pressure Plasma Jet-Assisted Synthesis of Zeolite-Based Low-k Thin Films. *ACS Applied Materials & Interfaces*, **10**(1); 900–908

Hussein, N. K. and S. Kadhem (2021). The Optical Properties of C\Mg, Nano-Rods Produced by the Explosion wire Technique. *Journal of Physics: Conference Series*, **2114**(1); 012041

Jung, E. Y., C. S. Park, H. J. Jang, S. Iqbal, T. E. Hong, B. J. Shin, M. Choi, and H. S. Tae (2022). Optimization of Atmospheric Pressure Plasma Jet with Single-Pin Electrode Configuration and Its Application in Polyaniline Thin Film Growth. *Polymers*, **14**(8); 1535

Kinandana, A. W., S. Sumariyah, and M. Nur (2018). Analysis of Plasma-Activated Medium (PAM) in Aqueous Solution by an Atmospheric Pressure Plasma Jet (APPJ). *MATEC Web of Conferences*, **197**; 02013

Lee, G. W. (2013). Phase Transition Characteristics of Flame-Synthesized Gamma-Al_2O_3 Nanoparticles with Heat Treatment. *International Journal of Materials and Metallurgical Engineering*, **7**(9); 699–702

Mikailzade, F., F. Önal, M. Maksutoglu, M. Zarbali, and A. Göktaş (2018). Structure and Magnetization of Polycrystalline $La_{0.66}Ca_{0.33}MnO_3$ and $La_{0.66}Ba_{0.33}MnO_3$ Films Prepared Using Sol-Gel Technique. *Journal of Superconductivity and Novel Magnetism*, **31**; 4141–4145

Mohammed, R. S., K. A. Aadim, and K. A. Ahmed (2022). Synthesis of CuO/ZnO and MgO/ZnO Core/Shell Nanoparticles with Plasma Gets and Study of Their Structural and Optical Properties. *Journal of Modern Science*, **8**(2); 9

Nikiforov, A. Y., C. Leys, M. Gonzalez, and J. Walsh (2015). Electron Density Measurement in Atmospheric Pressure

Plasma Jets: Stark Broadening of Hydrogenated and Non-Hydrogenated Lines. *Plasma Sources Science and Technology*, **24**(3); 034001

Parauha, Y. R., V. Sahu, and S. Dhoble (2021). Prospective of Combustion Method for Preparation of Nanomaterials: A Challenge. *Materials Science and Engineering: B*, **267**; 115054

Riyadh, S. M., K. D. Khalil, and A. H. Bashal (2020). Structural Properties and Catalytic Activity of Binary Poly (Vinyl Alcohol)/Al_2O_3 Nanocomposite Film for Synthesis of Thiazoles. *Catalysts*, **10**(1); 100

Sathish, S. and B. C. Shekar (2012). Transparent Nano Composite Thin Films for Thin Film Transistors and Opto-Electronic Devices. *Applications of Nano Materials: Electronics, Energy and Environment*; 289–296

Segawa, H., H. Okano, K. Wada, and S. Inoue (2014). Fabrication of Alumina Films with Laminated Structures by Ac Anodization. *Science and Technology of Advanced Materials*, **15**(1); 014209

Shameli, K., M. B. Ahmad, S. D. Jazayeri, S. Sedaghat, P. Shabanzadeh, H. Jahangirian, M. Mahdavi, and Y. Abdollahi (2012). Synthesis and Characterization of Polyethylene Glycol Mediated Silver Nanoparticles by the Green Method. *International Journal of Molecular Sciences*, **13**(6); 6639–6650

Sugumaran, S., C. S. Bellan, and M. Nadimuthu (2015). Characterization of Composite PVA–Al_2O_3 Thin Films Prepared by Dip Coating Method. *Iranian Polymer Journal*, **24**; 63–74

Tanaka, S., D. Inao, K. Hasegawa, K. Hokamoto, P. Chen, and X. Gao (2021). Graphene Formation through Pulsed Wire Discharge of Graphite Strips in Water: Exfoliation Mechanism. *Nanomaterials*, **11**(5); 1223

Tang, C. M., Y. H. Tian, and S. H. Hsu (2015). Poly (Vinyl Alcohol) Nanocomposites Reinforced with Bamboo Charcoal Nanoparticles: Mineralization Behavior and Characterization. *Materials*, **8**(8); 4895–4911

Ussenov, Y. A., M. T. Toktamyssova, M. K. Dosbolayev, M. T. Gabdullin, T. T. Daniyarov, and T. S. Ramazanov (2021). Thin-Film Deposition by Combining Plasma Jet with Spark Discharge Source at Atmospheric Pressure. *Contributions to Plasma Physics*, **61**(3); e202000140

Yadav, S. and P. K. Bajpai (2018). Effect of Substrate on CuS/PVA Nanocomposite Thin Films Deposited on Glass and Silicon Substrate. *Soft Nanoscience Letters*, **8**(2); 9–19

Yang, Z., D. Xu, J. Liu, J. Liu, L. Li, L. Zhang, and J. Lv (2015). Fabrication and Characterization of Poly (Vinyl Alcohol)/Carbon Nanotube Melt-Spinning Composites Fiber. *Progress in Natural Science: Materials International*, **25**(5); 437–444

Zhao, X., G. Wei, X. Meng, and A. Zhang (2014). High Performance Alumina Films Prepared by Direct Current Plus Pulse Anodisation. *Surface Engineering*, **30**(7); 455–459